

# Constraining Venus' convection regime from Baltis Vallis topography

Nathan J. McGregor<sup>1</sup> (nmcgregor@ucsc.edu), F. Nimmo<sup>1</sup>, C. Gillmann<sup>2</sup>, G. J. Golabek<sup>3</sup>, A. M. Plattner<sup>4</sup>, and J. W. Conrad<sup>5</sup>

<sup>1</sup>University of California Santa Cruz, Santa Cruz, CA, <sup>2</sup>Rice University, Houston, TX, <sup>3</sup>University of Bayreuth, Bayreuth, Germany, <sup>4</sup>University of Alabama, Tuscaloosa, AL, <sup>5</sup>NASA Marshall Space Flight Center, Huntsville, AL

## 1. Is a stagnant-lid or heat-pipe model a better representation of heat transport on Venus?

**MOTIVATION:** Baltis Vallis (BV) is a 6,800-km long lava channel on Venus with a present-day uphill flow direction. A 2000-km wavelength has been identified in its power spectrum whose length scale is comparable to the thickness of Venus' mantle, suggesting that mantle convection is responsible for the observed deformation (Conrad et al., 2021). Older studies suggest Venus has a surface age of 300 Myr to 1 Gyr (Hauck et al., 1998; McKinnon et al., 1997); however, recent estimates yield a younger surface age of 150 to 240 Myr (Herrick and Rumpf, 2011; Le Feuvre and Wiczorek, 2011). BV's deformation indicates that mantle convection was active over this timeframe.

**SIGNIFICANCE:** We place constraints on Venus' present-day internal structure and dynamics by comparing dynamical topography produced by simulated mantle convection with the observed topography of BV.

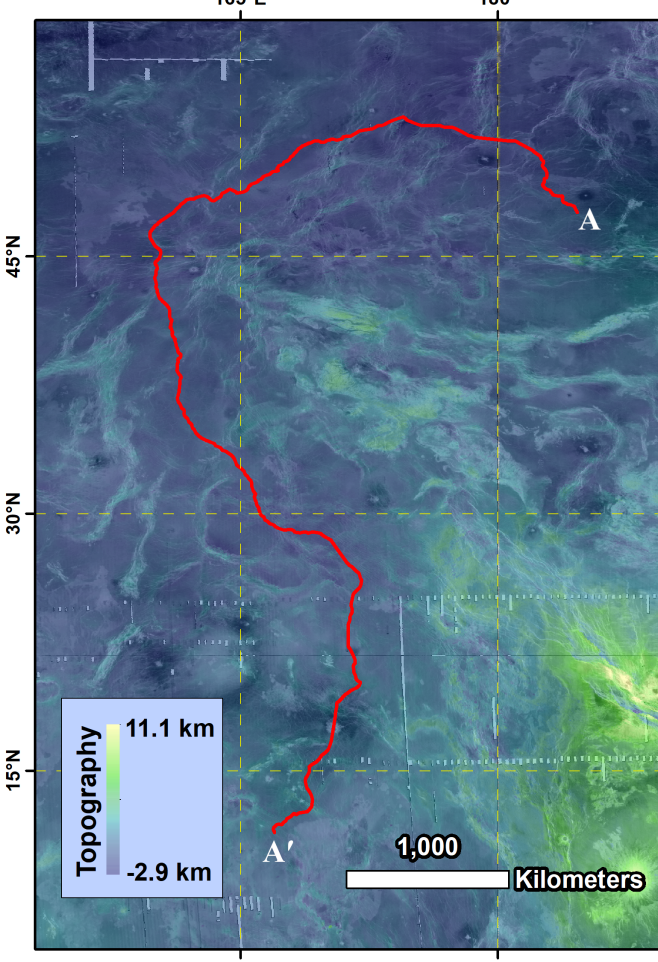


Figure 1. Topographic map of BV. A and A' mark the inferred source and termination points, respectively (Baker et al., 1992).

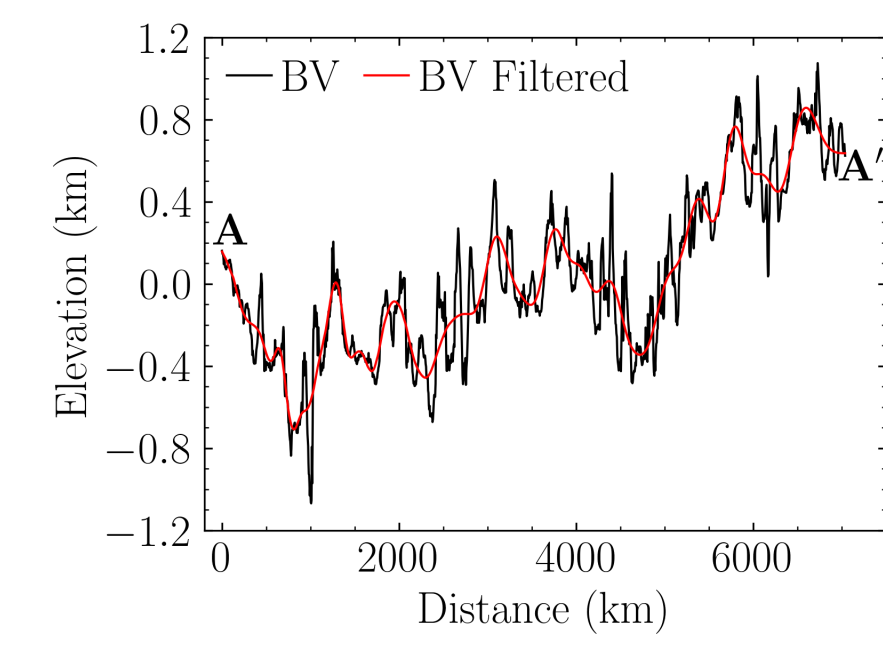


Figure 2. BV's original and filtered topographic profiles. Short wavelengths are removed to highlight long-wavelength deformation caused by mantle convection.

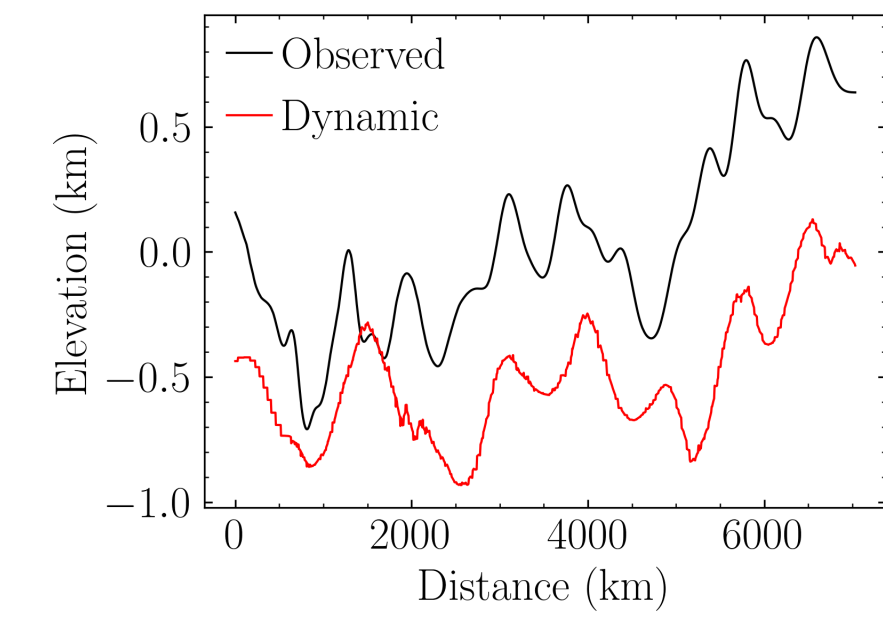


Figure 3. BV's observed and dynamic topographic profiles. The latter is derived from gravity data ( $\ell=65$ ) using the admittance between gravity and elevation (McKenzie, 1994).

## 2. Observable metrics

**MODELS:** We simulate time-dependent stagnant-lid mantle convection on Venus with a suite of coupled interior-surface evolution models for a range of assumed mantle properties using the StagYY code (Tackley, 2008; Gillmann et al., 2014).

**METRICS:** We compare the topographies of model BV profiles to the observed topography of BV using two metrics: **root-mean-square (RMS) height** and **decorrelation time**. The decorrelation time is inspired by the observation of BV's present-day uphill flow and the inference that the present-day topography must be uncorrelated with the original topography when BV formed flowing downhill.

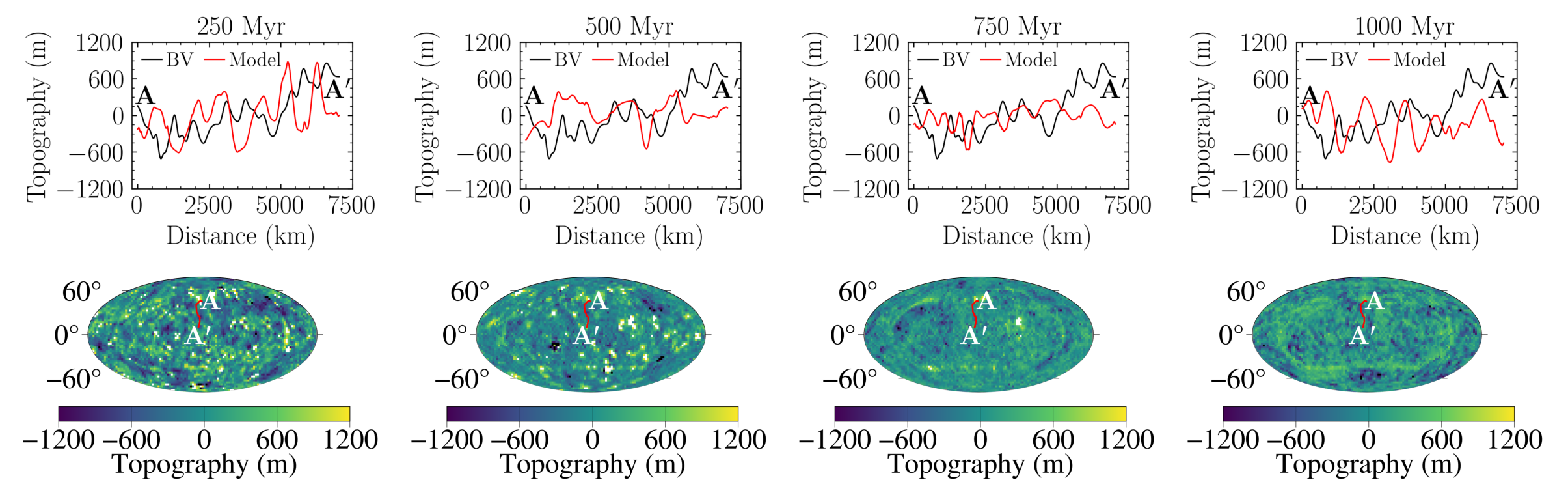


Figure 4. Shown are time steps depicting the surface topographic evolution from model VL3. Above, we plot the filtered BV and model topographic profiles above. Below, we plot the model dynamic topography across Venus' surface with BV indicated.

**FAVORED MODELS: VL3 and L3** have an RMS height similar to BV's RMS height and a decorrelation time less than Venus' surface age.

## 3. Constraining Venus' convection regime

### 3.1 Viscosity Profile

- The viscosity of Venus' lower mantle in VL3 and L3 is  $\sim 10^{20}$  Pa s, two orders of magnitude lower than Earth's.

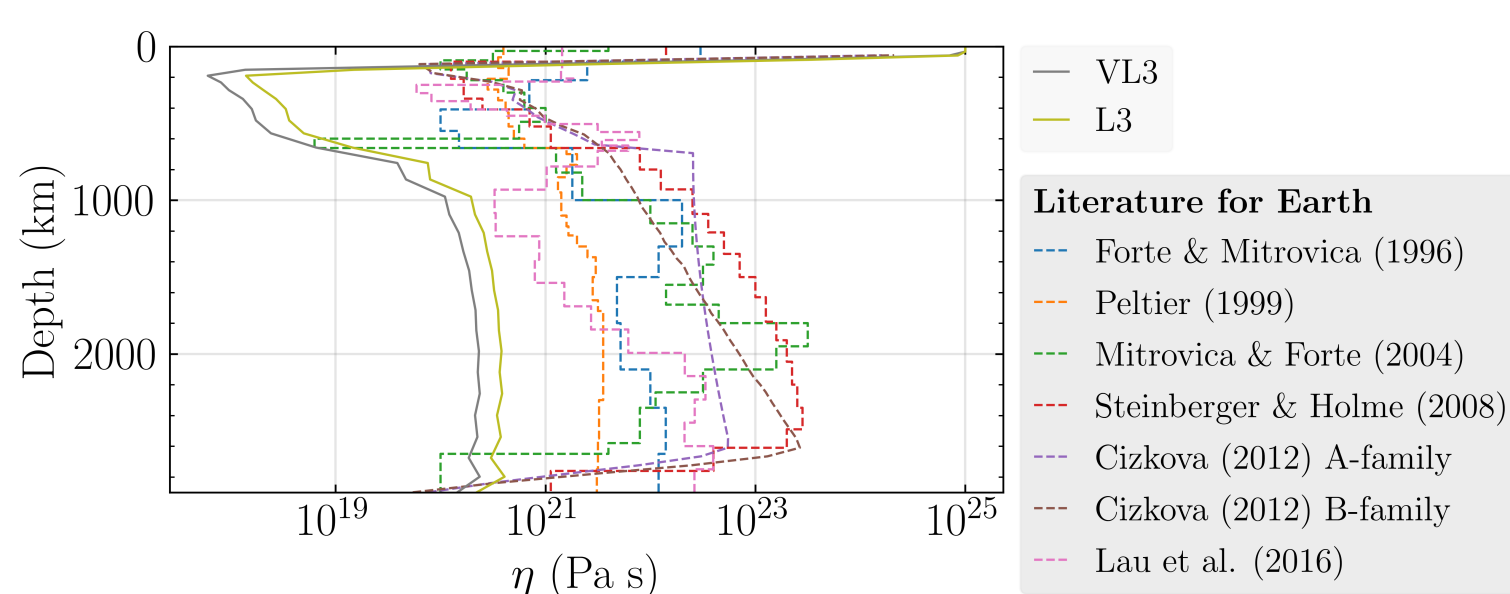


Figure 5. Solid lines are radial viscosity profiles for Venus for VL3 and L3. Dashed lines are radial viscosity profiles for Earth from previous studies.

### 3.3 Heat Fluxes

- Our model fluxes are consistent with inferred heat fluxes from previous studies (Smrekar et al., 2012; 2022).  
- VL3 and L3 have some of the highest heat fluxes, largely due to melt advection.

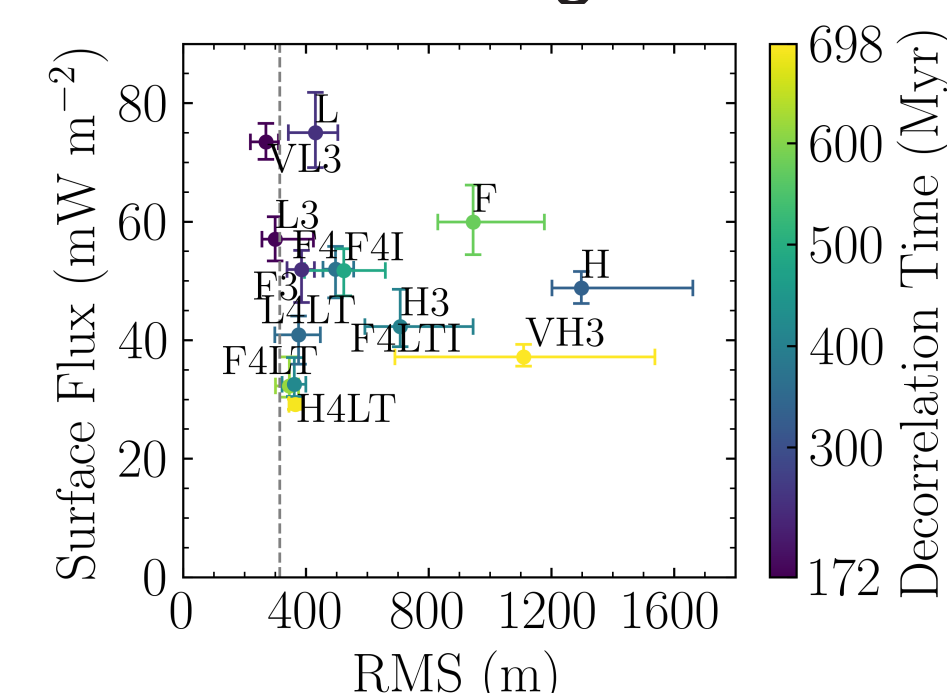


Figure 8. Total surface heat fluxes and RMS heights colored by decorrelation time. BV's RMS height is plotted as a dashed line. Error bars are interquartile ranges.

### 3.2 Decorrelation Time

- Models with higher total surface heat fluxes yield lower decorrelation times.  
- The shortest decorrelation times are associated with high  $Ra$ .

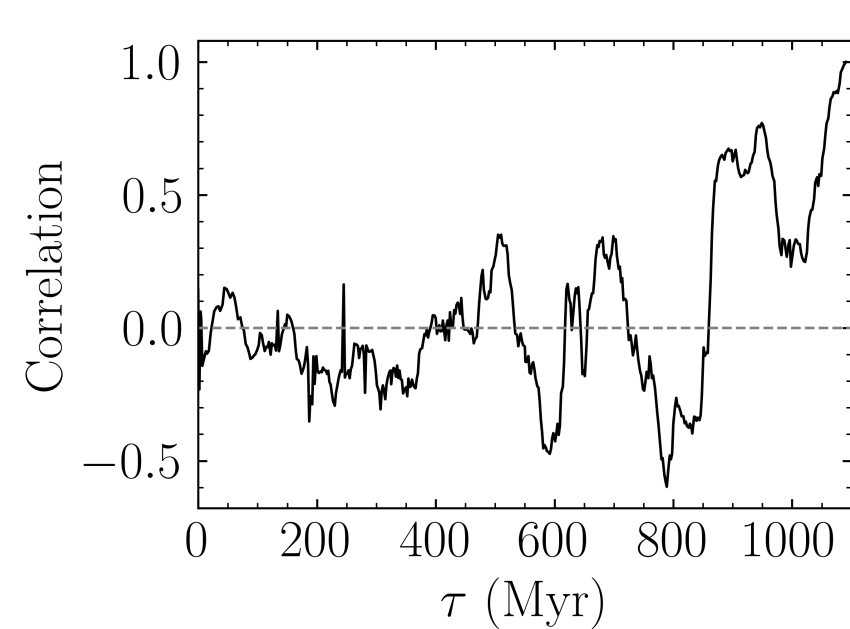


Figure 6. Correlation as a function of model time  $\tau$  for VL3. The dashed line indicates the cutoff value of zero. The correlation between model BV topography at a later time  $\tau_2$  and an earlier time  $\tau_1$  is calculated. When this correlation first falls to zero, the **decorrelation time** is then  $\tau_2 - \tau_1$  (Fig. 7).

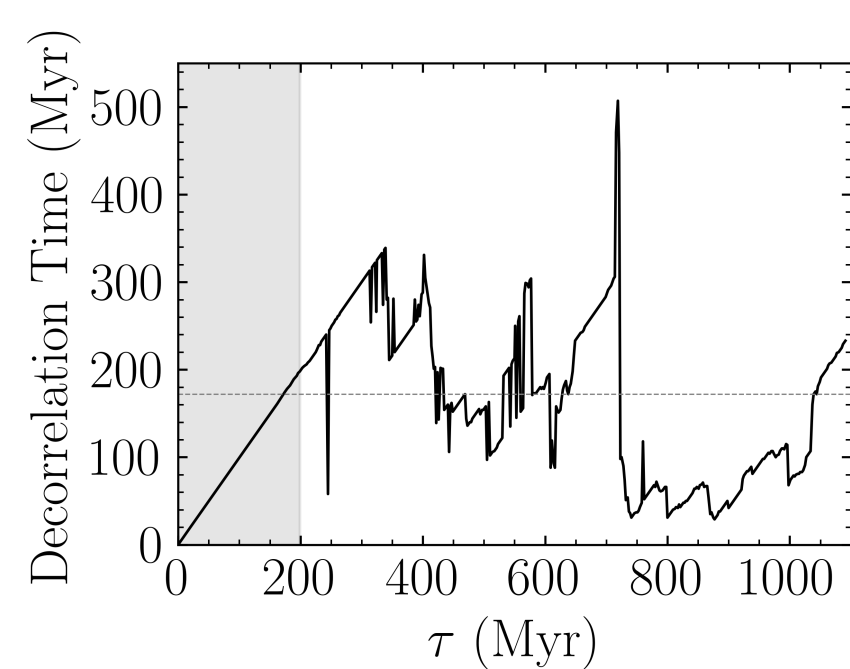


Figure 7. Decorrelation time as a function of model time  $\tau$  for VL3. The dashed line indicates the median decorrelation time for VL3. The shaded region represents the first 200 Myr of simulated mantle evolution that is excluded from consideration to allow the simulations to stabilize.

### 3.4 RMS Height

- Models with a higher  $Ra$  have a lower RMS height (Guimond et al., 2022).  
- Models with a lower RMS value have a shorter decorrelation time.

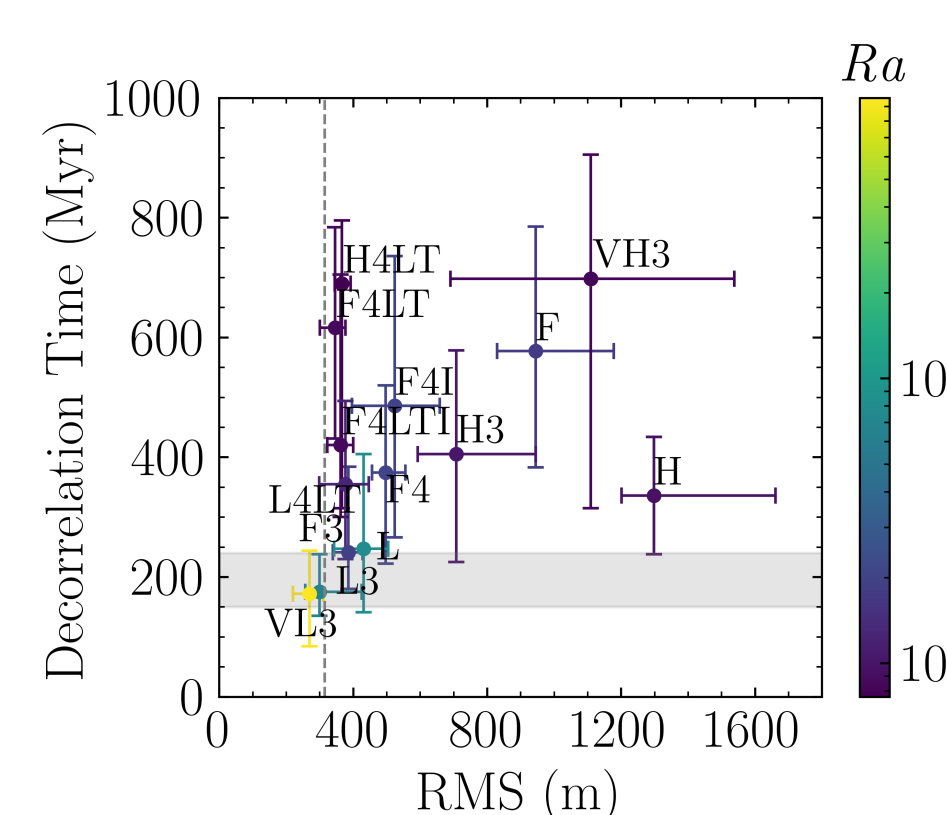


Figure 9. Decorrelation times and RMS heights colored by  $Ra$ . The dashed line denotes BV's RMS height. The shaded region indicates recent estimates for Venus' surface age (Herrick and Rumpf, 2011; Le Feuvre and Wiczorek, 2011). Error bars are interquartile ranges.

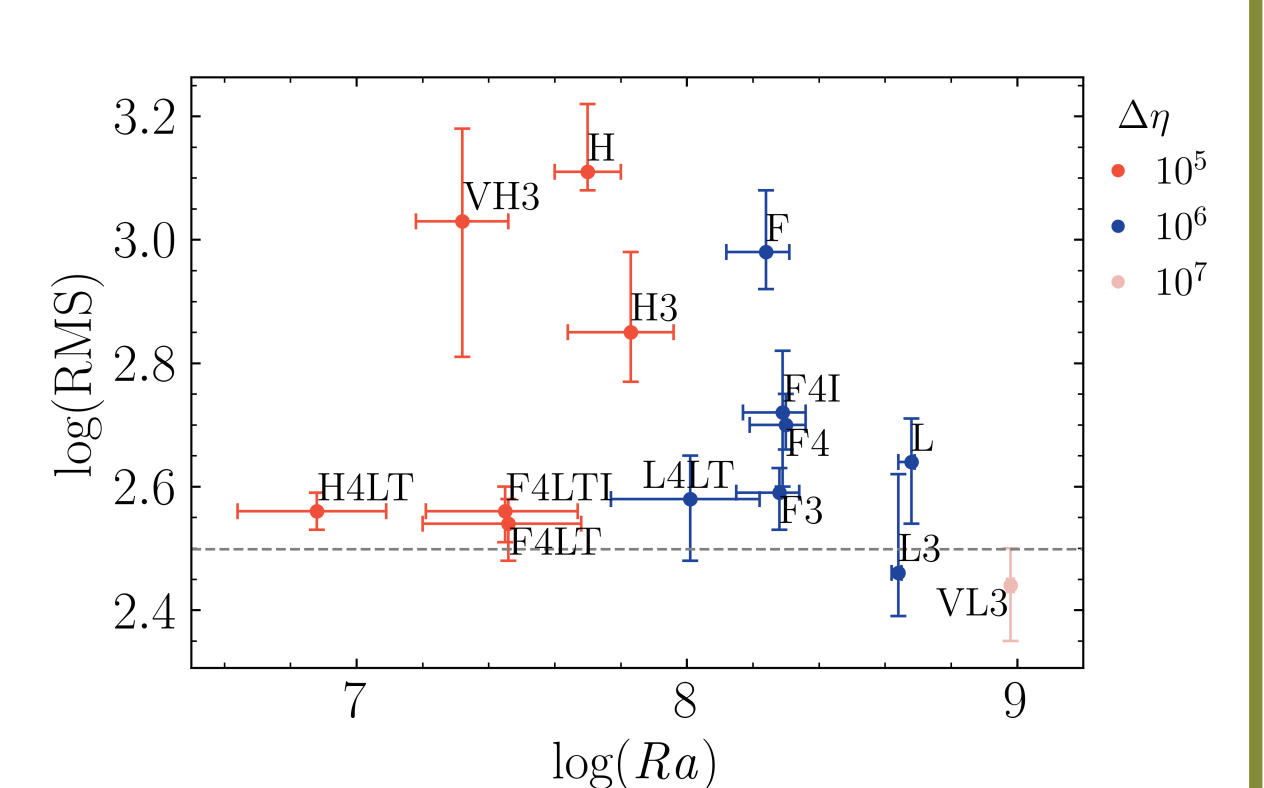


Figure 10. RMS heights and  $Ra$ . Color indicates the order of magnitude of the median viscosity contrast for each model. BV's RMS height is plotted as a dashed line. Error bars indicate interquartile ranges.

## 4. A heat-pipe mechanism may be operating on Venus

- From 14 mantle convection models, each initialized with different parameters, we identified **two convection models (VL3 and L3) that best fit our metrics**.  
- Our favored models have **low RMS heights, short decorrelation times, vigorous convection, high surface heat fluxes, and a lower viscosity profile than Earth's**.  
- The majority of the surface heat flux in our models is due to melt advection, indicating **high rates of volcanic resurfacing**.  
- If a heat-pipe mechanism is operating on Venus, then the **standard thermal profiles used to calculate elastic thickness may need to be reevaluated**.

## 5. Favored model properties

	Decorrelation Time (Myr)	RMS (m)	$Ra_e$	$\Delta\eta$
L3	$175^{+63}_{-40}$	$300^{+125}_{-43}$	$4.34^{+0.13}_{-0.18} \times 10^8$	$7.11^{+0.04}_{-0.14} \times 10^6$
VL3	$172^{+72}_{-88}$	$270^{+41}_{-50}$	$9.65^{+0.20}_{-0.27} \times 10^8$	$1.73^{+0.04}_{-0.06} \times 10^7$
BV		315		

Table 1. Properties of our favored models and Baltis Vallis: Decorrelation Time; RMS height; Effective Rayleigh Number,  $Ra_e$ ; Viscosity Contrast,  $\Delta\eta$ . Lower and upper errors indicate the range to the first and third quartiles, respectively.